# Influence of the Degree of Swelling on the Stiffness and Toughness of Microgel-Reinforced Hydrogels

*Michael Kessler, Tianyu Yuan, John M. Kolinski, and Esther Amstad\**

The stiffness and toughness of conventional hydrogels decrease with increasing degree of swelling. This behavior makes the stiffness-toughness compromise inherent to hydrogels even more limiting for fully swollen ones, especially for load-bearing applications. The stiffness-toughness compromise of hydrogels can be addressed by reinforcing them with hydrogel microparticles, microgels, which introduce the double network (DN) toughening effect into hydrogels. However, to what extent this toughening effect is maintained in fully swollen microgel-reinforced hydrogels (MRHs) is unknown. Herein, it is demonstrated that the initial volume fraction of microgels contained in MRHs determines their connectivity, which is closely yet nonlinearly related to the stiffness of fully swollen MRHs. Remarkably, if MRHs are reinforced with a high volume fraction of microgels, they stiffen upon swelling. By contrast, the fracture toughness linearly increases with the effective volume fraction of microgels present in the MRHs regardless of their degree of swelling. These findings provide a universal design rule for the fabrication of tough granular hydrogels that stiffen upon swelling and hence, open up new fields of use of these hydrogels.

## 1. Introduction

Hydrogels are networks made from polymers that are connected through crosslinks[1] and contain a large fraction of water.[2] Unfortunately, the swelling of conventional gel networks significantly reduces their mechanical properties. For example, the strain at break[3] and modulus[4,5] of a conventional hydrogel decrease with increasing degree of swelling.[6] Their fracture toughness decreases even more rapidly upon swelling as it scales with their areal swelling ratio.[3,7] The decrease in fracture toughness upon swelling measured for conventional hydrogels is in good agreement with the observation by Lake and Thomas for rubbers, whose fracture toughness scales with the areal density of polymer chains that transverse the fracture plane.[8] This scaling is particularly limiting for hydrogels because they are often used under physiological conditions where they swell, such that their density of polymer chains decreases and hence their stiffness and toughness decrease.[9–11] This limitation restricts the use of hydrogels to fields that do not require any load-bearing properties and solely demand soft, highly swellable components, such as contact lenses or diapers. To partially address this limitation, hydrogels have been functionalized with thermo-sensitive monomers that do not swell within a certain temperature range to counteract their swelling.[12,13] However, the counter-action to the swelling only works within a limited temperature range.

An established design strategy to improve the resistance to fracture of swollen hydrogels is to introduce energy dissipative mechanisms into them.[14] Prominent examples for tough hydrogels are double network hydrogels (DNs), which consist of a first, highly crosslinked and brittle network, and a second, loosely crosslinked and stretchy one.[15] Upon fracture of DNs, the first, sacrificial network dissipates a significant amount of energy via breakage of covalent[15–18] or ionic[19] bonds, while the second network maintains the mechanical integrity of the material. The design principle is universal, and has been transferred to solvent-free multinetwork elastomers.[20,21] The toughening of DNs arises from the breakage of bonds in the first network, as has been demonstrated by mechano-radical polymerization in hydrogels[22,23] and with mechanophores that were covalently incorporated into multinetwork elastomers.[24] These results indicate that the breakage of bonds within the first, sacrificial network is confined to a damage zone that surrounds advancing cracks. The fracture toughness of DNs linearly scales with the size of this damage zone.[25–27] The yield point of DNs, which indicates the onset of major damage in the first network, arises at a yield stress that is inversely proportional to the areal swelling ratio of DNs, whereas the yield strain is inversely proportional to their linear swelling ratio.[28] However, traditional DNs are

M. Kessler, T. Yuan, E. Amstad
Soft Materials Laboratory
Institute of Materials
École Polytechnique Fédérale de Lausanne (EPFL)
Lausanne 1015, Switzerland
E-mail: esther.amstad@epfl.ch
J. M. Kolinski
Engineering Mechanics of Soft Interfaces Laboratory
Institute of Mechanical
Engineering, École Polytechnique Fédérale de Lausanne
(EPFL)
Lausanne 1015, Switzerland

**ADVANCED
SCIENCE NEWS**

www.advancedsciencenews.com

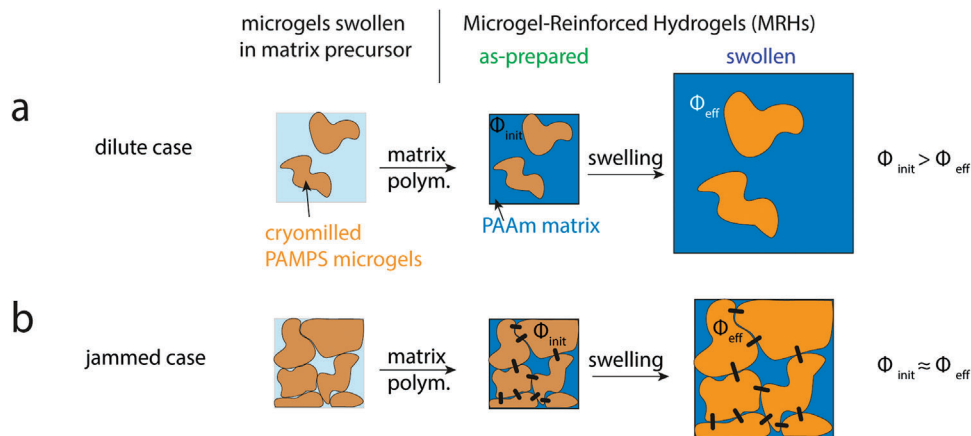**Macro-
molecular
Rapid Communications**

www.mrc-journal.de

**Figure 1.** Schematic illustration of the swelling of microgel-reinforced hydrogels (MRHs) that depends on the initial microgel volume fraction, $\phi_{init}$. a,b) The matrix precursor solution containing fully swollen microgels (left) is polymerized to form a bulk hydrogel, which is subsequently tested as prepared (center), or fully swollen in water (right). a) If the microgels are initially in the dilute regime, the degree of swelling of MRHs depends on that of the matrix, microgels, and the microgel volume fraction. In this case, the effective microgel volume fraction decreases upon swelling, $\phi_{init} > \phi_{eff}$. b) If the microgels are in contact with each other during the polymerization of the matrix, they are firmly connected and these connections remain intact even when MRHs are fully swollen. In this case, the swelling is dependent on the swelling of the microgels only and $\phi_{eff} \approx \phi_{init}$.

limited in terms of processing, as their first network must be swollen in the precursor solution of the second network, thereby sacrificing the control over the shape of the final sample.[15,16] To overcome this limitation, and to couple excellent toughness and stiffness with advanced processability, microgels have been embedded into single-network hydrogels to form microgel-reinforced hydrogels (MRHs) that feature the double network toughening effect.[29] Microgels are hydrogel microparticles of any shape that have at least one dimension between 0.1 and 1000 µm.[10,30] They are swollen in the precursor solution of the second network, herein called matrix, before they are brought into shape via molding,[29] or, at high microgel volume fractions, 3D printing.[31] The matrix is subsequently polymerized to form tough MRHs. The toughness of MRHs is most strongly influenced by the microgel volume fraction and the molar ratio of the two networks within the microgels.[32] Unfortunately, little is known about how the bulk swelling of MRHs influences their stiffness and fracture toughness. Insights into this correlation would enable the targeted design of tough MRHs that can be cast or 3D printed into complex, well-defined 3D shapes without significantly weakening them in their swollen state.

In this work, we study the effect of the bulk swelling of MRHs on their stiffness and fracture toughness. We demonstrate that the initial poly(2-acrylamido-2-methyl-1-propanesulfonic acid sodium salt) (PAMPS) microgel volume fraction in MRHs before swelling governs the connectivity of the microgels: if the microgel volume fraction is in the dilute regime, the matrix freely swells because microgels are individually dispersed, as illustrated in **Figure 1**a. If, however, the microgel volume fraction enters the semidilute regime, adjacent particles start to be in contact with each other such that during the polymerization of the matrix, they are firmly interconnected, as shown in Figure 1b. These firm inter-particle links reduce the degree of swelling of MRHs, and hence increase their stiffness in the swollen state. We assign this behavior to a swelling-induced strain-stiffening effect of the PAMPS polyelectrolyte network that makes up the firmly interconnected microgels. In contrast, the fracture toughness of

MRHs is much less dependent on the connectivity between microgels, and is independent of their size. Instead, it linearly scales with the effective microgel volume fraction in MRHs. These findings relate the fracture toughness of MRHs to their microstructure and provide design rules for tough granular hydrogels that stiffen upon swelling.

## 2. Results and Discussion

### 2.1. Fabrication and Swelling of MRHs

We reinforce poly(acrylamide) (PAAm) hydrogels with PAMPS microgels. To achieve this goal, we produce a bulk PAMPS hydrogel that we break into fragments with dimensions ranging from 1 to 1000 µm using a commercial cryo-miller.[9] We employ cryo-milling to produce microgels because this technique has a much higher throughput and shorter processing time than the more commonly used emulsification techniques that require several washing steps. Yet, the higher throughput of the cryo-miller comes at the expense of the control over the shape and size of microfragments. We swell the obtained microgels in water and freeze-dry them to obtain a powder that is easily dispersible in aqueous solutions. We subsequently swell a known weight of dried microgels in a defined volume of an aqueous matrix precursor solution, which contains acrylamide (AAm) monomers, $N, N'$-methylene bisacrylamide (MBAA), a crosslinker, and a photoinitiator. By precisely controlling the weight of added microgels we tune the volume fraction of the microgels contained within MRHs. To transform the swollen microgels into MRHs, we polymerize the reagents contained in the aqueous precursor solution by exposing these samples to ultraviolet (UV) light.

The stiffness of MRHs strongly depends on the microgel volume fraction.[29] To convert the known weight fraction of microgels into a volume fraction of microgels in the as-prepared and swollen states, we perform confocal microscopy on our MRHs. To facilitate visualization of the microgels, we fluorescently label them with a positively charged dye, cresyl violet, as exemplified
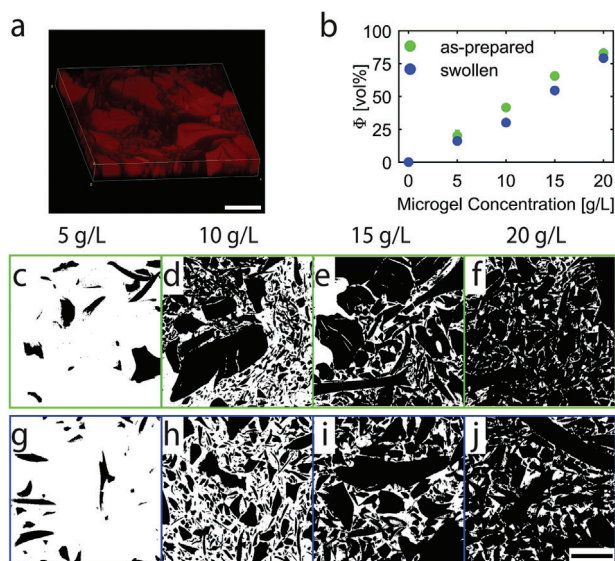
**ADVANCED
SCIENCE NEWS**

www.advancedsciencenews.com

Macro-
molecular
Rapid Communications

www.mrc-journal.de

**Figure 2.** Microgel volume fractions. a) Confocal microscopy image of an as-prepared MRH reinforced with 10 g L$^{-1}$ microgels that have been stained with cresyl violet. Scale bar = 100 μm. b) Microgel volume fraction Φ as a function of the microgel concentration. c–h) Thresholded z-slices of c–f) as-prepared and g–j) swollen MRHs reinforced with various weight fractions of microgels. Scale bar = 200 μm.

in **Figure 2**a.[33] The actual volume fractions of microgels are calculated from z-stack confocal images, as exemplified on thresholded z-slices of as-prepared and swollen MRHs shown in Figure 2c–j. The volume fraction of as-prepared MRHs, $\phi_{init}$, linearly increases with increasing mass of added microgels, as demonstrated in Figure 2b. By contrast, the volume fraction of swollen MRHs, $\phi_{eff}$, nonlinearly increases with the microgel volume fraction, especially at higher microgel concentrations, as shown in Figure 2b. We assign this nonlinear trend to the confinement of microgels that are in the semidilute regime: If microgels are in the dilute state, they are not confined by their neighboring microgels such that they are individually dispersed and swell much less than the surrounding matrix. As a result, the effective microgel volume fraction in the swollen state, $\phi_{eff}$, is lower than $\phi_{init}$, as schematically illustrated in Figure 1a. By contrast, if the microgel concentration exceeds 20 g L$^{-1}$, where they enter the semidilute state, they are in contact with neighboring microgels such that the swelling of the surrounding matrix is hindered, as exemplified in Figure 2j. This result suggests microgels that have been dispersed in the semidilute regime are firmly connected such that they form a percolating network that presents the analogue of the first fully crosslinked network in DNs.[34] In this case, the swelling of the microgels is constrained such that their swelling is similar to the bulk swelling of MRHs and hence, $\phi_{eff} \approx \phi_{init}$, as illustrated in Figure 1b.

If microgels that are dispersed in the semidilute regime indeed form a percolating network, we expect the degree of swelling of MRHs to plateau above a threshold value of $\phi_{init}$. To test this expectation, we quantify the degree of swelling of as-prepared and fully swollen MRHs by comparing their sample weights. The weight of PAAm gels increases 3.9-fold upon swelling. Assuming a polymer density of 1 g cm$^{-3}$, the volume of pure PAAm

gels also increases 3.9-fold upon swelling. Indeed, the degree of swelling of MRHs containing low volume fractions of microgels decreases with increasing $\phi_{init}$, until it plateaus, as shown in **Figure 3**a. Interestingly, the swelling ratio of an MRH with $\phi_{init} = 83 \pm 1$ vol% is within experimental error the same as that of a bicontinuous bulk double network hydrogels, even though the polymer fraction contained within the swollen DN is significantly higher than that contained in the MRH sample, as shown in Figure 3b. This result suggests that MRHs with $\phi_{init} \geq 83 \pm 1$ vol% possess a DN-like structure due to the connectivity between the microgels, which restrains their swelling. Note that we observe a similar trend in swelling ratios for MRHs containing smaller fragmented microgels and even for those containing spherical microgels, as shown in Figure S1 (Supporting Information). This comparison implies that the swelling ratio and the inter-particle connections are mainly influenced by the volume fraction of the microgels, and not by their size or shape.

If microgels form inter-particle connections when initially dispersed in the semidilute regime, their inter-particle contact area should increase upon the formation of the 2$^{nd}$ network. To test if this is indeed the case, we prepare large, spherical, monodisperse microgels using microfluidics, as detailed in the Supporting Information. These microgels are processed into MRHs containing 20 g L$^{-1}$ monodisperse microgels such that the microgels are in the semidilute regime.[35] We subsequently let the MRHs swell freely and visualize the samples using optical microscopy. Despite the swelling, the microgels are nonspherical and show pronounced inter-microgel contact areas, as shown in Figure 2c, indicating that the microgels are indeed linked to each other. We assign the inter-particle bonds to the presence of reactive groups at the microparticle surface that can be used to form covalent inter-particle bonds during the radical polymerization of the second network. A similar effect can be found in DNs, as reactive groups are present in the first network and can be further crosslinked with the second network.[34] Note that the initial volume fractions of the nonspherical, cryo-milled microgels are very similar to those of spherical microgels that can be determined using a simple calibration curve,[35] as summarized Figure S2 (Supporting Information). This result indicates the microgel volume fraction is independent of the microgel shape.

The dense packing of the microgels leads to the formation of a single, percolating first hydrogel network, making MRHs a microstructured analogue of DNs, with the microgel network as the first network, and the matrix as the second. Yet, because of the nature of microgels, these formulations can easily be cast into well-defined shapes or even 3D-printed, in stark contrast to bulk DNs.

## 2.2. The Influence of the MRH Swelling on their Stress at Break and Extensibility

Our swelling results show that the initial microgel volume fraction $\phi_{init}$ determines the connectivity of reinforcing microgels, and hence the microstructure of the resulting MRHs. To assess how the microstructure influences the strength and extensibility of MRHs we perform tensile tests on fully swollen and as-prepared samples, as exemplified in Figure S3 (Supporting Information). While as-prepared MRHs display higher stress at break, $\sigma_b$, compared to fully swollen ones, the trends of as-prepared
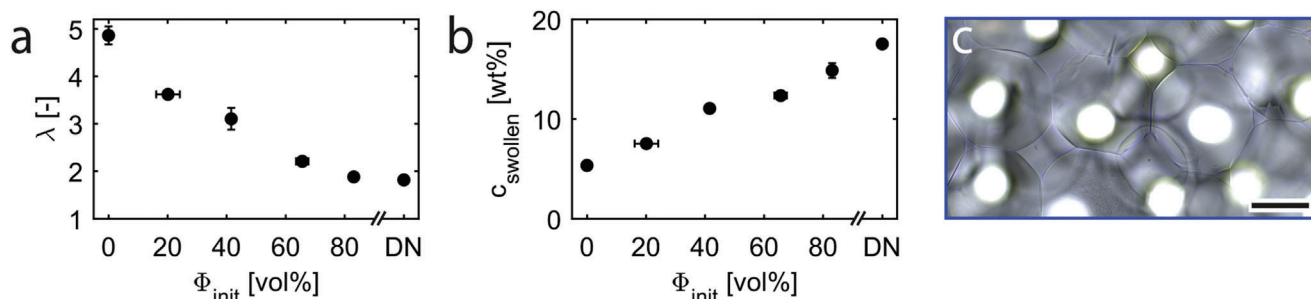
**Figure 3.** Volumetric swelling of microgel-reinforced hydrogels (MRHs). a) Volumetric swelling ratio $\lambda$ and b) polymer content in the swollen state as a function of the initial microgel volume fraction prior to swelling, $\phi_{init}$. c) Micrograph of a fully swollen hydrogel sheet reinforced with large, monodisperse microgels. Scale bar = 200 μm.
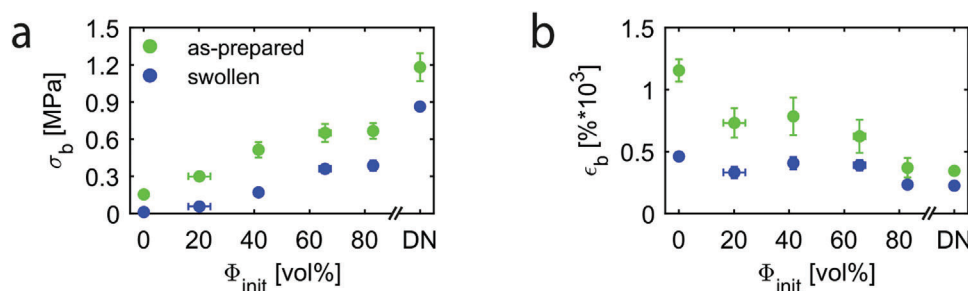


**Figure 4.** a) Stress at break $\sigma_b$, and b) strain at break $\epsilon_b$ as a function of the initial microgel volume fraction prior to swelling, $\phi_{init}$, for MRHs and DNs in their as-prepared (green) and fully swollen (blue) state.

and fully swollen MRHs as a function of $\phi_{init}$ are very similar, as shown in **Figure 4**a. Similarly, as-prepared MRHs show a slightly higher strain at break, $\epsilon_b$, compared to fully swollen ones. Yet the trend of the decreasing $\epsilon_b$ with increasing $\phi_{init}$ is very similar for both sample types, as shown in Figure 4b. Note that the size of the microgels does not significantly influence $\sigma_b$ or $\epsilon_b$ of the as-prepared MRHs, as detailed in Figure S4 (Supporting Information). Similarly, the microgel shape does not significantly influence the mechanical properties of as-prepared MRHs, as a comparison of the results we obtain here with those obtained on MRHs possessing the same overall composition but that are made of spherical microparticles, shown in Figure S5 (Supporting Information), reveals.[35] These results imply that $\sigma_b$ and $\epsilon_b$ are mainly determined by the hydrogel microstructure, which is governed by the microgel connectivity, and hence $\phi_{init}$. The initial microgel volume fraction is hence an important design parameter for the strain and stress at break of MRHs. Moreover, our results suggest that the swelling can be considered as prestretching of the polymer segments that does not change the mechanism of rupture of MRHs.[5]

## 2.3. The Influence of the MRH Swelling on their Stiffness

The stiffness of hydrogels depends on the volumetric density of elastically active strands, and therefore decreases with increasing swelling ratio.[1] Hence, we expect our MRHs to soften when swollen to equilibrium. To properly assess the effect of the swelling on the stiffness of MRHs, we use the effective microgel volume fraction in the swollen state, $\phi_{eff}$. The Young's modulus,

$E$, of as-prepared MRHs linearly increases with $\phi_{init}$. This linear correlation is in stark contrast to that observed for fully swollen samples where $E$ increases much slower with $\phi_{eff}$ if samples contain $\phi_{init} < 42 \pm 0$ vol% but increases much more steeply if $\phi_{init} > 42 \pm 0$ vol%, as shown in **Figure 5**a. Remarkably, MRHs with $\phi_{init} > 66 \pm 2$ vol% become stiffer upon swelling, a behavior that is in stark contrast to conventional bulk hydrogels which soften upon swelling.[1] A similar swelling-induced stiffening effect is observed for bulk DN hydrogels, as indicated in Figure 5a, which further proves the structural similarities between bulk DN hydrogels and MRHs with $\phi_{init} > 66 \pm 2$ vol%. These results are in good agreement with our findings from rheology tests, which revealed the onset of PAMPS microgel jamming at $\phi_{init} \geq 60$ vol%.[32] At these high microgel volume fractions, microparticles are covalently connected, resulting in a fully percolating first PAMPS network.

Hydrogels typically soften upon swelling. By contrast, we observe a stiffening upon swelling for MRHs with $\phi_{init} > 66 \pm 2$ vol% and DN hydrogels. We assign this behavior to the swelling-induced prestretch of the PAMPS network. Indeed, polyelectrolyte gels, like PAMPS hydrogels used here, experience a discontinuous increase in modulus when prestretched through swelling to equilibrium in a solution containing low salt concentrations.[36] By analogy, the DN-like structure of MRHs containing densely packed, firmly interlinked microgels stiffens upon swelling due to a prestretching of PAMPs chains contained within and between the micro-fragments. Remarkably, despite the increase in stiffness, the fracture toughness of these materials is still considerable, at least 1 kJ m$^{-2}$, a feature that is difficult to obtain in conventional hydrogels.[37,38]
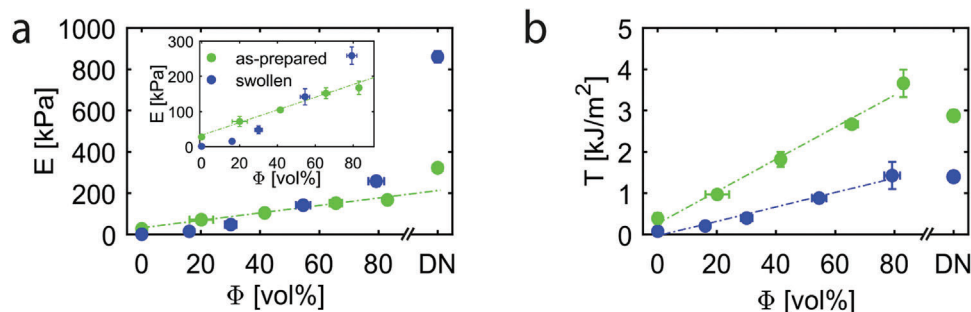
**ADVANCED
SCIENCE NEWS**

www.advancedsciencenews.com

[M]acro-molecular
Rapid Communications

www.mrc-journal.de

**Figure 5.** Influence of the effective microgel volume fraction $\phi_{eff}$ on the stiffness and fracture toughness of microgel-reinforced hydrogels (MRHs). a) Young's modulus $E$ and b) fracture toughness $T$ of MRHs in their as-prepared (green) and fully swollen (blue) state as a function of $\phi_{eff}$. a,b) The dashed lines are linear fits to the experimental data.

### 2.4. The Influence of the Swelling of MHRs on their Fracture Toughness

The fracture energy in tough hydrogels is the sum of the intrinsic energy required to break polymer chains within the crack plane, and the energy dissipated in the damage zone surrounding the crack plane.[39] The fracture toughness of conventional hydrogels is proportional to the intrinsic chain scission energy, and scales linearly with the areal polymer chain density and hence decreases with their areal degree of swelling.[3,7] However, for tough hydrogels with multiple networks, the fracture toughness also includes energy dissipation in the damage zone around the crack front, which arises from damage within the sacrificial networks.[16] Consequently, the linear correlation between the fracture toughness and the areal polymer chain density no longer holds. To examine which condition better describes our MRHs, we quantify the influence of the degree of swelling of MRHs on the fracture toughness $T$ using simple extension tests (SETs), as detailed in the Supporting Information. We mathematically account for the stretch in the sample legs, as the fixation of inextensible strips onto them was inhibited by their surface rugosity. The fracture toughness of as-prepared samples linearly increases with $\phi_{eff}$, as shown in Figure 5b. Note that $T$ of the pure PAAm that does not contain any microgels, is slightly higher than what we would expect from the linear trend of the $T(\phi_{init})$ dataset. We assign the higher fracture toughness of as-prepared microgel-free PAAm samples to the presence of entangled polymer chains that are freely dispersed in the network and hence, can be removed during the washing step. Interestingly, swollen MRHs also display a linear relation between $T$ and $\phi_{eff}$, as shown in Figure 5b. This linear relationship between the fracture toughness and the volume fraction of microgels of MRHs is in contrast to the linear trend between the fracture toughness and the areal polymer density measured for conventional hydrogels. Indeed, regions reinforced with microgels in MRHs can be seen as DNs at micrometer scales, and the energy can hence be dissipated by breaking the sacrificial PAMPS chains in the microgels.[29] The identical scaling for as-prepared and fully swollen MRHs indicates that the network architecture of MRHs and their degree of inter-microgel connectivity do not influence their fracture toughness. Instead, this scaling suggests that the fracture toughness of MRHs mainly depends on the volumetric density of PAMPS chains within the damage zone at the crack front, which is analogous to the frac-
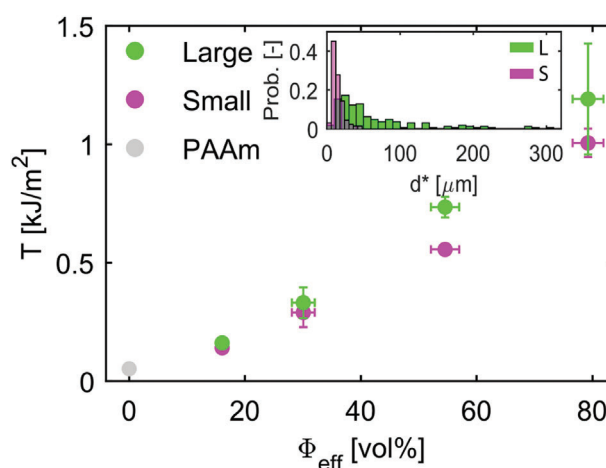


**Figure 6.** Fracture toughness $T$ of fully swollen MRHs reinforced with large (green) or small (magenta) microgels as a function of the effective microgel volume fraction, $\phi_{eff}$. The inset is the size distribution of large (green) and small (magenta) microgels.

ture toughness of tough multinetwork hydrogels. To confirm this suggestion, we perform SETs on MRHs reinforced with large microgels that display a wide size distribution and those reinforced with small microgels displaying a narrow size distribution. We do not measure a significant difference between samples reinforced with these two types of microgels, as shown in **Figure 6**, confirming that the size and uniformity of the microgels do not affect the toughness of MRHs.

## 3. Conclusion

Microgel-reinforced hydrogels have the potential to combine the double network toughening mechanism with excellent processability. Here, we demonstrate that hydrogels that are reinforced with high volume fractions of microgels swell much less than what would be expected from the rule of mixture. We assign this deviation from linearity to strong inter-microgel connections that form if adjacent microgels are in contact when the second polymer network is formed, thereby restricting the swelling of the second network. These firm inter-microgel links strongly increase the stiffness of MRHs upon swelling, a behavior that

ADVANCED
SCIENCE NEWS

www.advancedsciencenews.com

[M] acro-
molecular
Rapid Communications

www.mrc-journal.de

is unusual for conventional hydrogels. In contrast, the fracture toughness decreases with an increasing degree of swelling and is linearly related to the effective microgel volume fraction present in the material. These correlations provide clear guidelines for the design of tough microgel-reinforced hydrogels that stiffen upon swelling. Importantly, thanks to the presence of microgels in the precursor solution, they can be processed into well-defined 3D shapes through casting, or even 3D printing if they contain high microgel volume fractions without compromising the mechanical properties of MRHs.

## Supporting Information

Supporting Information is available from the Wiley Online Library or from the author.

## Conflict of Interest

The authors declare no conflict of interest.

## Data Availability Statement

The data that support the findings of this study are available from the corresponding author upon reasonable request.

[1] C. Creton, *Macromolecules* **2017**, *50*, 8297.
[2] O. Wichterle, D. Lím, *Nature* **1960**, *185*, 117.
[3] X. Zhao, X. Chen, H. Yuk, S. Lin, X. Liu, G. Parada, *Chem. Rev.* **2021**, *121*, 4309.
[4] P. J. Flory, *Principles of Polymer Chemistry*, Cornell University Press, Ithaca, NY **1953**.
[5] K. Hoshino, T. Nakajima, T. Matsuda, T. Sakai, J. Ping Gong, *Soft Matter* **2018**, *14*, 9693.
[6] M. C. Boyce, E. M. Arruda, *Rubber Chem. Technol.* **2000**, *73*, 504.
[7] Y. Akagi, H. Sakurai, J. P. Gong, U. Chung, T. Sakai, *J. Chem. Phys.* **2013**, *139*, 144905.
[8] G. J. Lake, A. G. Thomas, D. Tabor, *Proc. R. Soc. London, Ser. A* **1967**, *300*, 108.
[9] H. Yuk, J. Wu, T. L. Sarrafian, X. Mao, C. E. Varela, E. T. Roche, L. G. Griffiths, C. S. Nabzdyk, X. Zhao, *Nat. Biomed. Eng.* **2021**, *5*, 1131.
[10] A. C. Daly, L. Riley, T. Segura, J. A. Burdick, *Nat. Rev. Mater.* **2020**, *5*, 20.
[11] H. Yuk, C. E. Varela, C. S. Nabzdyk, X. Mao, R. F. Padera, E. T. Roche, X. Zhao, *Nature* **2019**, *575*, 169.
[12] H. Kamata, Y. Akagi, Y. Kayasuga-Kariya, U. Chung, T. Sakai, *Science* **2014**, *343*, 873.
[13] G. Chen, K. Hou, N. Yu, P. Wei, T. Chen, C. Zhang, S. Wang, H. Liu, R. Cao, L. Zhu, B. S. Hsiao, M. Zhu, *Nat. Commun.* **2022**, *13*, 7789.
[14] X. Zhao, *Soft Matter* **2014**, *10*, 672.
[15] J. P. Gong, Y. Katsuyama, T. Kurokawa, Y. Osada, *Adv. Mater.* **2003**, *15*, 1155.
[16] J. P. Gong, *Soft Matter* **2010**, *6*, 2583.
[17] T. Nakajima, T. Kurokawa, S. Ahmed, W. Wu, J. P. Gong, *Soft Matter* **2013**, *9*, 1955.
[18] Y. Jia, Z. Zhou, H. Jiang, Z. Liu, *J. Mech. Phys. Solids* **2022**, *169*, 105090.
[19] J.-Y. Sun, X. Zhao, W. R. K. Illeperuma, O. Chaudhuri, K. H. Oh, D. J. Mooney, J. J. Vlassak, Z. Suo, *Nature* **2012**, *489*, 133.
[20] P. Millereau, E. Ducrot, J. M. Clough, M. E. Wiseman, H. R. Brown, R. P. Sijbesma, C. Creton, *Proc. Natl. Acad. Sci. USA* **2018**, *115*, 9110.
[21] E. Ducrot, C. Creton, *Adv. Funct. Mater.* **2016**, *26*, 2482.
[22] T. Matsuda, R. Kawakami, T. Nakajima, J. P. Gong, *Macromolecules* **2020**, *53*, 8787.
[23] Y. Chen, G. Sanoja, C. Creton, *Chem. Sci.* **2021**, *12*, 11098.
[24] E. Ducrot, Y. Chen, M. Bulters, R. P. Sijbesma, C. Creton, *Science* **2014**, *344*, 186.
[25] Y. Tanaka, R. Kuwabara, Y.-H. Na, T. Kurokawa, J. P. Gong, Y. Osada, *J. Phys. Chem. B* **2005**, *109*, 11559.
[26] Y. Tanaka, *EPL* **2007**, *78*, 56005.
[27] H. R. Brown, *Macromolecules* **2007**, *40*, 3815.
[28] T. Matsuda, T. Nakajima, Y. Fukuda, W. Hong, T. Sakai, T. Kurokawa, U. Chung, J. P. Gong, *Macromolecules* **2016**, *49*, 1865.
[29] J. Hu, K. Hiwatashi, T. Kurokawa, S. M. Liang, Z. L. Wu, J. P. Gong, *Macromolecules* **2011**, *44*, 7775.
[30] T. I. U. of P. and A. Chemistry, (IUPAC), "IUPAC - microgel (M03901)," https://doi.org/10.1351/goldbook.M03901. https://goldbook.iupac.org/terms/view/M03901. (accessed: October, 2022).
[31] M. Hirsch, A. Charlet, E. Amstad, *Adv. Funct. Mater.* **2020**, *31*, 2005929.
[32] J. Hu, T. Kurokawa, K. Hiwatashi, T. Nakajima, Z. L. Wu, S. M. Liang, J. P. Gong, *Macromolecules* **2012**, *45*, 5218.
[33] I. L. H. Ong, E. Amstad, *Small* **2019**, *15*, 1903054.
[34] T. Nakajima, H. Furukawa, Y. Tanaka, T. Kurokawa, Y. Osada, J. P. Gong, *Macromolecules* **2009**, *42*, 2184.
[35] M. Kessler, Q. Nassisi, E. Amstad, *Macromol. Rapid Commun.* **2022**, *43*, 2200196.
[36] M. Rubinstein, R. H. Colby, A. V. Dobrynin, J.-F. Joanny, *Macromolecules* **1996**, *29*, 398.
[37] Z. Li, Z. Liu, T. Y. Ng, P. Sharma, *Extreme Mech. Lett.* **2020**, *35*, 100617.
[38] J. Tang, J. Li, J. J. Vlassak, Z. Suo, *Extreme Mech. Lett.* **2017**, *10*, 24.
[39] R. Bai, J. Yang, Z. Suo, *Eur. J. Mech. A: Solids* **2019**, *74*, 337.